Available online at www.sciencedirect.com
ScienceDirect
Journal of Catalysis 245 (2007) 205–214
JOURNAL OF CATALYSIS
www.elsevier.com/locate/jcat

Catalysis by doped oxides: CO oxidation by $Au_xCe_{1-x}O_2$

Vladimir Shapovalov, Horia Metiu *

Department of Chemistry and Biochemistry, University of California, Santa Barbara, CA 93106-9510, USA

Received 12 July 2006; revised 5 October 2006; accepted 5 October 2006

Abstract

Density functional theory calculations for the $CeO_2(111)$ surface doped with Au, Ag, and Cu show that the bond between the oxygen atoms and the oxide is weakened by presence of the dopant. In CO oxidation, doping of CeO_2 with Au allows the oxide to react readily with CO and make carbonates. These decompose to release CO_2 and form an oxygen vacancy on the surface. The vacancy adsorbs oxygen from the gas and weakens its bond, so that it reacts with CO to form a carbonate, which decomposes to release CO_2 and heal the oxygen vacancy. To be a good oxidation catalyst, a doped oxide must achieve a balance between two conflicting requirements: It must make surface oxygen reactive but not so much that it will hinder the healing of the oxygen vacancies created by the oxidation reaction.

Keywords: Doped ceria; Carbon monoxide; Oxidation catalyst; DFT calculation

1. Introduction

It is well known that small gold clusters supported on various oxides catalyze the water–gas shift reaction at low temperature [1–15]. In a series of remarkable papers Fu, Deng, Salzburg, and Flytzani-Stephanopoulos [10,13–15] proposed that the catalytic activity in this system is due to gold ions and not to the neutral gold clusters. To show this, they prepared a Au/CeO_2 catalyst containing neutral gold clusters and measured the rate of the water–gas shift reaction catalyzed by it. Then they dissolved the gold clusters in a cyanide solution. After the metallic gold was removed, the system catalyzed the water–gas shift reaction as well as the original system did and had the same effective activation energy. Electron microscopy detected no gold clusters, and X-ray photoelectron spectroscopy (XPS) indicated the presence of Au^{3+}. The structure of the system, obtained by X-ray diffraction (XRD) measurements, is that of ceria with a slightly modified interatomic distance. Subsequent work [16] concluded that catalysis is performed by neutral gold; at present, the active site in this system is unclear.

Au supported on a various oxides is a good low-temperature CO oxidation catalyst [17–33]. Corma's group [34–36] has shown that the activity of Au supported on ceria increases with increasing Au^{3+}-to-Au^0 ratio. The presence of Au^{3+} was inferred from the vibrational frequency of CO adsorbed on the catalyst; that of CO adsorbed on Au^{3+} differs from that of CO adsorbed on Au^0. Venezia et al. [37] have used several methods for preparing a gold/ceria catalyst and have shown that the samples with no Au^0 had the highest activity for CO oxidation; 100% conversion was reached at lower temperatures than those used for the samples containing Au^0.

Recently Zhang et al. [38] prepared a Au/ZrO_2 catalyst and dissolved the neutral Au clusters in KCN. XPS measurements indicated that after dissolution, the sample contained Au^{3+}. This catalyst is very active and selective for partial hydrogenation of butadiene.

In the articles mentioned above, the nature of the active center was not established with certainty. We have proposed [39] that the active Au species is a gold atom that substitutes one of the cations in the host oxide and suggested that such substitution is a general method for modifying the reactivity of oxide-based catalysts. This proposal is consistent with experiments [40–49] that prepared single-phase oxides doped with different metal atoms to produce compounds with the formula $M_xN_{n-x}O_m$. Here M is the dopant, N is the cation of the host oxide (N_nO_m) and x is <0.2. The catalytic activity of several such compounds has been tested. $Cu_xCe_{1-x}O_2$ catalyzes

* Corresponding author. Fax: +1 (805) 893 4120.
E-mail address: metiu@chem.ucsb.edu (H. Metiu).

0021-9517/$ – see front matter
doi:10.1016/j.jcat.2006.10.009

[40] NO reduction with NH_3; $Pt_xCe_{1-x}O_2$ performs the water–gas shift reaction [41]; $Pt_xCe_{1-x}O_2$ [42], $Rh_xCe_{1-x}O_2$ [44], $Ti_xCe_{1-x}O_2$ [43] and $Ce_{1-x-y}Ti_xPt_yO_2$ [43] perform CO oxidation; $Fe_xCe_{1-x}O_2$ catalyzes N_2O decomposition [45]; and $Ce_{0.9}Cu_{0.1}O_2$ catalyzes the steam reforming of methanol [48]. In all of these systems, the doped oxide is a better catalyst than the pure oxide.

A group in Japan [50–53] has shown that several doped perovskites are good automotive catalysts; in particular, $LaPd_xFe_{1-x}O_3$ is a better catalyst than Pd supported on alumina. XRD measurements show that the system is active only when the perovskite structure is intact; if the system decomposes into different oxides, then the activity is lost.

However, doping does not always improve catalytic activity. Zhao and Gorte [54] have shown that $Sm_{0.2}Ce_{0.8}O_{1.9}$, $Gd_{0.2}Ce_{0.8}O_{1.9}$, $La_{0.2}Ce_{0.8}O_{1.9}$, $Nb_{0.1}Ce_{0.9}O_{2.05}$, and $Ta_{0.1}Ce_{0.9}O_{2.05}$ have lower activity for *n*-butane oxidation than ceria. Similar conclusions were reached by Wilkes et al. [55], who showed that the rate of CO oxidation by ceria doped with La, Pr, Gd, or Nb is lower than the rate of oxidation by pure ceria by a factor of 3–5.

Previously, we used density functional theory (DFT) to study CO oxidation by $Au_xTi_{1-x}O_2$ [39] and found the following: (1) The gold dopant prefers to substitute a five-coordinated Ti atom on the surface rather than go into the bulk; (2) the dopant weakens the bond between the surface oxygen atoms and the doped oxide, making it more reactive; (3) these oxygen atoms react with gas-phase CO to form a CO_2 molecule that readily desorbs; (4) the oxygen vacancy created by CO_2 removal adsorbs an oxygen molecule that reacts with CO to form a carbonate; (5) the carbonate decomposes easily to produce gaseous CO_2 and heal the oxygen vacancy; and (6) doping with Cu, Ag, Ni, Pd, or Pt weakens the oxygen bond to the surface more than doping with Au.

We extrapolate our findings and speculate that in most cases, doping weakens the bond of the oxygen atoms to the oxide, making them more reactive. This assumption has the following implications:

1. Oxides that perform oxidation or dehydrogenation reactions by a Mars–van Krevelen mechanism are likely to perform the same reactions at lower temperature if the oxide is doped.
2. Doped oxides require smaller amounts of expensive metals; for example, $LaPd_xFe_{1-x}O_3$ uses 70% less Pd than an ordinary supported Pd catalyst [50–53].
3. Sometimes the doped oxides have higher thermal stability than the ordinary supported catalyst. This is true for $LaPd_xFe_{1-x}O_3$ [50–53], but the stability of other doped oxides under reaction conditions remains a matter of debate [13,14].
4. Doped catalysts are more tunable than pure oxides, because x can be varied in $M_xN_{m-x}O_n$, and a given oxide can be paired with different dopants and a given dopant with various oxides.
5. The oxidation reaction has two critical steps: (1) removal of an oxygen atom by the reducing agent to form an oxygen vacancy and (2) reaction of this vacancy with gas-phase oxygen to annihilate the vacancy and prevent the complete reduction of the oxides. In a good oxidation catalyst, these 2 steps must be well balanced. If doping overweakens the bond of the surface–oxygen atom with the oxide, then the oxidation reaction (of, e.g., CO) is efficient, but the reoxidation of the vacancy is slow and the efficiency of the catalyst suffers.

In this work we use DFT calculations to examine CO oxidation by $CeO_2(111)$ surface doped with Au and compare the activity of the doped oxide with that of the pure oxide surface. Our focus is on the effect of the gold doping on the reaction pathway and on the formation and the stability of various carbonate intermediates detected spectroscopically. The main effect of doping is to activate the oxygen atoms on the surface of the oxide and to facilitate the formation of an oxygen vacancy during CO oxidation. Because of this, we have examined the energy of vacancy formation for ceria doped with Au, Ag, and Cu. Even though the oxides of Ag and Cu are more stable than those of Au, doping with Ag or Cu has an even greater destabilizing effect on surface oxygen than doping with Au.

2. Computational details

Ceria has been the subject of several DFT calculations [56–67], which determined the stability of various crystal faces and the energy of formation of oxygen vacancies at the surface. Hermansson's group calculated the adsorption of CO on ceria [68–70], and Nolan et al. [67] examined the adsorption of CO, NO_2, and NO.

Ceria has narrow f-bands, which is known to cause difficulties with some aspects of the electronic properties calculated by generalized gradient approximation (GGA) [71–86]. We believe that although there is cause for concern, there is no hard evidence that GGA gives unusually large errors when used to calculate the *energy differences* of interest to chemists. For example, we computed the energy of the reaction $CeO_{2,bulk} = (1/2)Ce_2O_{3,bulk} + (1/4)O_{2,gas}$ and found good agreement between GGA calculations using soft oxygen pseudopotentials (2.12 eV), those using hard oxygen pseudopotentials (1.95 eV), and experiment (1.97 eV) [87]. The value for experiment was the enthalpy at 0 K, calculated using available thermodynamic data [88]. Here we assume that the errors are such that our *qualitative* conclusions regarding the effect of the dopant on the chemistry of the oxide are valid. Exploratory calculations (V. Shapovalov and H. Metiu, unpublished data), including the on-site Coulomb repulsion (DFT + U), do not change the conclusions reached here.

The surface was modeled by a slab with six atomic layers, separated by 15 Å of vacuum. The atoms in the three bottom layers were frozen in the positions given by a GGA calculation of bulk CeO_2. We used a hexagonal supercell (Fig. 1) with a side length of 11.67 Å. The positions of all atoms in the top three layers of the slab and the adsorbate were optimized to give minimum energy.

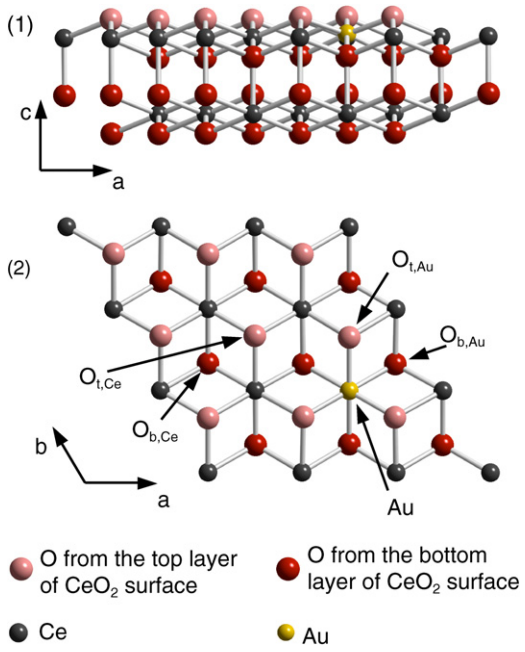

Fig. 1. Side (1) and top (2) views of the unit cell used in the calculations. We distinguish between the top (light red) and bottom (dark red) layer oxygen atoms. Corresponding atoms are given index "t" or "b." Further, if an O atom is bound to an Au atom, it is given index "Au." If an O atom is bound only to Ce atoms it is given index "Ce." Examples of differently bound oxygen atoms ($O_{t,Au}$, $O_{b,Au}$, $O_{t,Ce}$, and $O_{b,Ce}$) with respect to gold (Au) are pointed out.

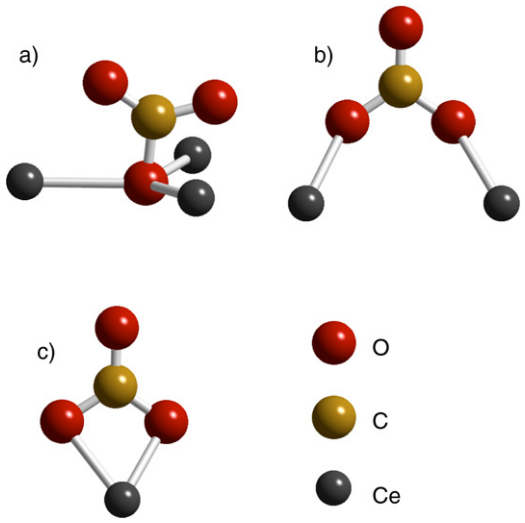

Fig. 2. Types of carbonates experimentally detected on the CeO_2 surface: (a) monodentate; (b) bridging; (c) bidentate.

To test the convergence of the calculations with respect to the slab thickness, we computed the surface energies for slabs having 6, 9, and 12 atomic layers. The surface energies were 1.66, 1.66, and 1.64 eV per CeO_2 formula unit, respectively. This indicates that the six-layer slab provides converged surface properties. The composition of the slab used in our calculations was $Ce_{18}O_{36}$ or $Au_1Ce_{17}O_{36}$, corresponding to the approximate stoichiometric formula $Au_{0.06}Ce_{0.94}O_2$ or, equivalently, atomic % Au = 5.6 (i.e., 1 × 100/18). Many experiments [40–49] have been performed with $M_xCe_{1-x}O_2$ (where M is the dopant) with $x \leqslant 0.2$. Other experiments [10,11,15,34,35,89] used an Au concentration of around 0.5–5 atom% and as high [37] as 12 atom% (8 wt%). It was also experimentally observed that the surface concentration of Au on CeO_2 crystallites is 10–16 times higher than the bulk concentration [40,89]. Thus, the concentration of Au in our model was within the experimental range.

The calculations were performed using the VASP 4.5 program [90–93] with PAW pseudopotentials and the rPBE functional. We included in the calculations 11 electrons for Au, 12 electrons for Ce, 6 electrons for O, and 4 electrons for C atoms. All calculations were spin-polarized, but the spin–orbit coupling was neglected. The plane-wave cutoff energy was 374.9 eV. The convergence criterion for energy in the electronic and geometry minimizations was 10^{-4} eV. We used Gaussian smearing at the Fermi level with width $\sigma = 0.05$. Due to the large size of the cell, we calculated the energy at the Γ-point only.

To describe various structures formed by CO adsorption on $Au_xCe_{1-x}O_2$, we used the following nomenclature. The top three atomic layers, starting from the vacuum side, contain oxygen, cerium, and oxygen, respectively. The index "t" indicates the oxygen atoms in the top layer and "b" indicates those in the second layer. In addition, the index "Au" identifies the oxygen atoms bound to both Au and Ce atoms and "Ce" identifies those bound to Ce atoms only. For example, $O_{b,Au}$ is an oxygen atom located in the second O layer and in the first coordination shell of Au.

The reaction energy differences reported here are the energies of the products minus the energies of the reactants; a negative reaction energy corresponds to an exothermic process.

3. Results

We examined the energy changes caused by various processes that we consider likely participants in the reaction mechanism. We mention only those that are thermodynamically important, although we have tried all reasonable possibilities. Because we do not calculate activation energies, these results are pertinent to a system in thermodynamic equilibrium.

3.1. CO oxidation involving an oxygen atom nearest to the gold dopant

A CO molecule can adsorb on an oxide surface in various ways. It may form a bond with the surface and maintain its identity, with its bond length and vibrational frequency close to those of gas-phase CO; it can bind strongly to an oxygen atom and form a molecule with bond length and vibrational frequency close to those of CO_2 (this species could be thought of as a CO_2 molecule adsorbed at an oxygen-vacancy site); or it could form a monodentate, bridging, or bidentate carbonate (see Fig. 2).

In this section we examine the sequence of events that follow the reaction of a CO molecule with an oxygen atom nearest to Au. On the $Au_xCe_{1-x}O_2(111)$ surface, we find that CO reacts with two oxygen atoms neighboring the Au dopant to form the carbonate shown in Fig. 3b. In this figure, the green ball is

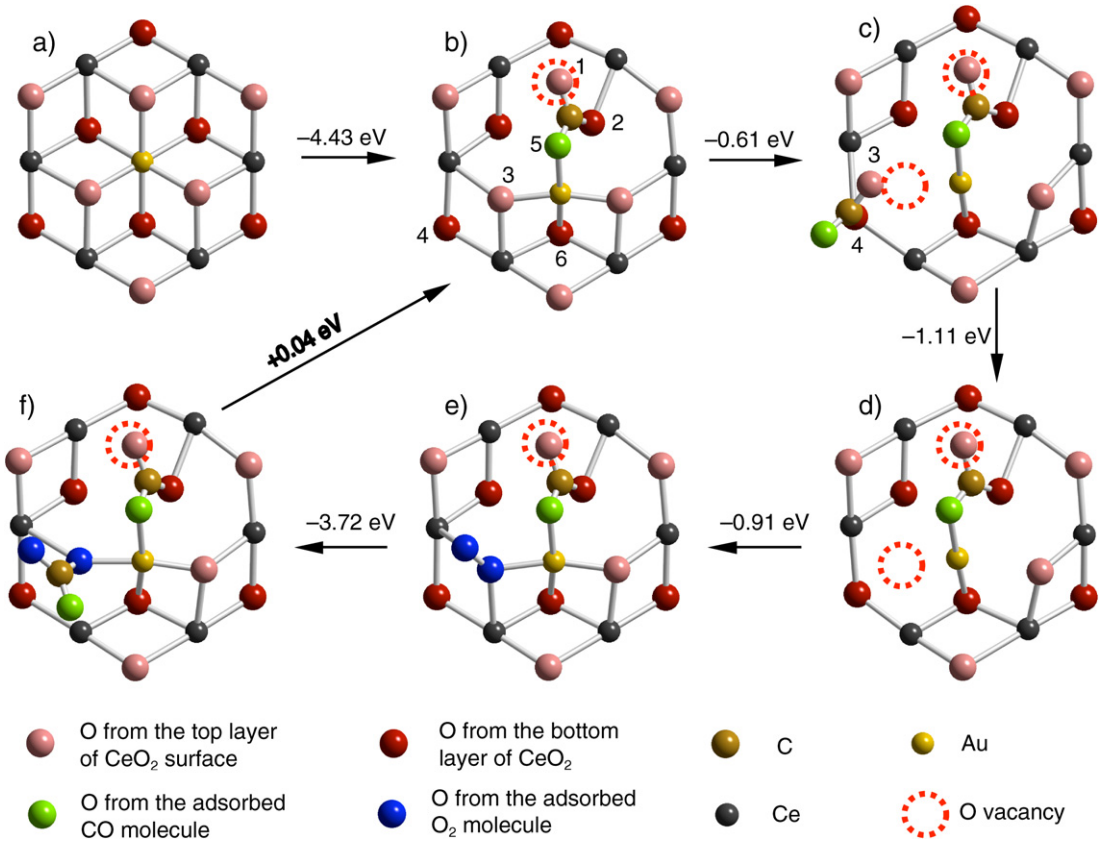

Fig. 3. CO oxidation in the vicinity of a Au atom: (a) clean surface; (b) formation of the spectator carbonate. O vacancy is formed at this step, but it is staggered with the carbonate O in this view; (c) formation of the second carbonate; (d) CO_2 desorbed leaving an O vacancy; (e) adsorption of O_2 at the vacancy; (f) formation of carbonate with adsorbed O_2; (b) CO_2 desorbed.

the oxygen atom from CO. The carbonate is formed by binding the carbon atom to the $O_{t,Au}$ (atom 1) and $O_{b,Au}$ (atom 2). The $O_{t,Au}$ (atom 1) is pulled out of its site to create an oxygen vacancy, indicated by a dotted circle. The oxygen atom from the CO binds to the gold dopant. This reaction is very exothermic (4.43 eV).

The bridging carbonate, formed by adsorbing CO on doped ceria, is rather stable; it takes 0.91 eV to remove CO_2 from the carbonate into the gas phase and leave behind an oxygen vacancy. Because oxygen-vacancy formation near the dopant is facile, this high exothermicity is due mostly to the stability of the carbonate. We expect that this carbonate will be present on the surface during catalysis. If the system is heated to a high temperature, this carbonate will decompose to produce gaseous CO_2 and an oxygen vacancy on the surface. This vacancy adsorbs O_2, which will react with CO to make a carbonate, which will decompose to form CO_2 and heal the oxygen vacancy. This sequence of reactions is catalytic, but it is not an efficient CO-oxidation pathway because the decomposition of the first carbonate is highly endothermic. This means that we must look for an alternative path.

It turns out that a second carbonate can form while the first is still present (Fig. 3c), by binding CO to $O_{b,Ce}$ oxygen (atom 4) and $O_{t,Au}$ (atom 3). The oxygen atom 3 is pulled out of its lattice site to create an oxygen vacancy, which is shown as a dotted circle (Fig. 3c). The formation of this carbonate is exothermic by 0.61 eV. Its decomposition, to produce gaseous CO_2 and an oxygen vacancy (Fig. 3d) near the Au atom, is exothermic by 1.11 eV.

The vacancy formed by the decomposition of the second carbonate adsorbs an oxygen molecule from the gas phase (Fig. 3e), with an exothermicity of 0.91 eV. The bond length of the adsorbed molecule is longer than that of gas-phase O_2, indicating that the π^* orbital of O_2 is populated and the bond in O_2 is weakened. However, the dissociation of the adsorbed O_2 molecule is endothermic and is not a factor in the catalytic process. The adsorbed O_2 reacts with gas-phase CO to form a carbonate (Fig. 3f) with an exothermicity of 3.72 eV. It takes very little energy (0.04 eV) to decompose this carbonate into a gaseous CO_2 molecule. This decomposition provides an oxygen atom that heals the oxygen vacancy at which the O_2 molecule was adsorbed. The system returns to the state shown in Fig. 3b.

As a result of this catalytic cycle, the surface consumes one O_2 molecule and two CO molecules to produce two CO_2 molecules; the carbonate formed first (Fig. 3b) is a spectator. One could say that the catalyst is the doped oxide with the first carbonate on it (Fig. 3b). To determine on which sites a CO molecule will form a carbonate, we check which two oxygen atoms on the surface are separated by a distance that is close to the distance by which they would be separated in a carbonate. There are three such oxygen-atom pairs: (3, 4), (3, 5), and (3, 6)

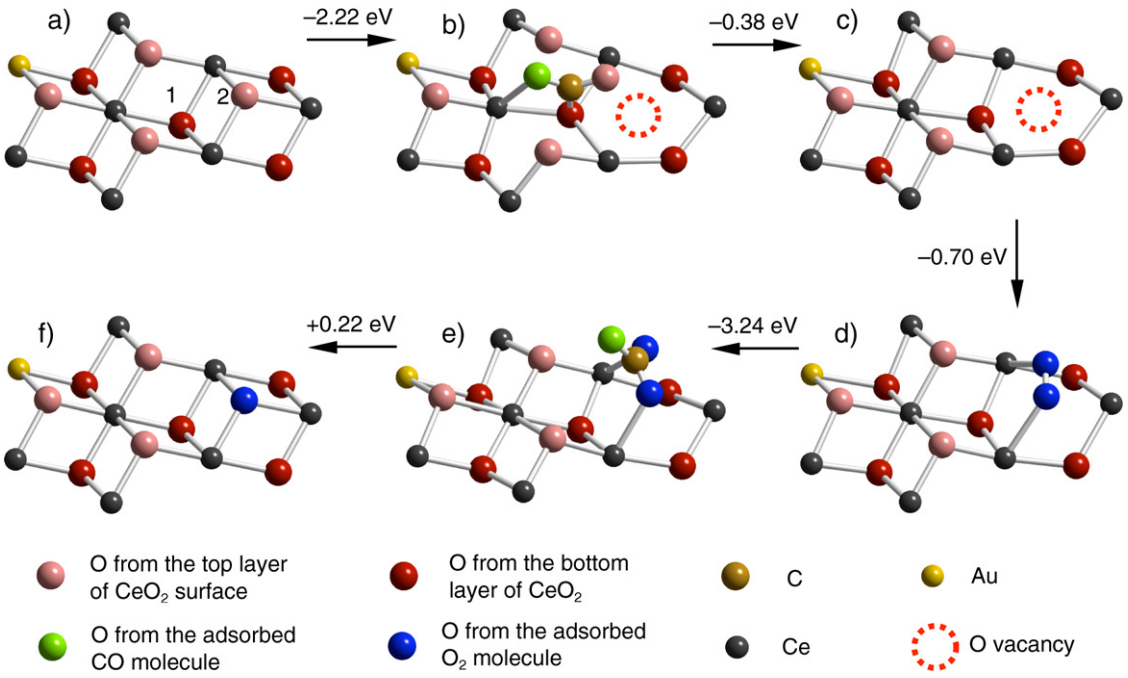

Fig. 4. CO oxidation away from the Au atom: (a) clean surface; (b) formation of carbonate; (c) CO_2 desorbed leaving an O vacancy; (d) adsorption of O_2 at the vacancy; (e) formation of carbonate with adsorbed O_2; (f) CO_2 desorbed, clean surface restored.

(see Fig. 3b). We found that the CO does not form a carbonate with the last two pairs.

3.2. CO oxidation involving an oxygen atom next-nearest to the gold dopant

We have also performed calculations to determine the activity of oxygen atoms located outside the first coordination shell of the dopant. The steps in the catalytic cycle involving such an oxygen atom are shown in Fig. 4. The oxygen atoms 1 and 2 (Fig. 4a) react with CO to form a bidentate carbonate (Fig. 4b). This reaction is exothermic by 2.22 eV and creates an oxygen vacancy by pulling the oxygen atom 2 out of its place; the location of the vacancy is shown by the dotted line. This carbonate decomposes to form gaseous CO_2 and an oxygen vacancy (Fig. 4c), with an exothermicity of 0.38 eV. Oxygen adsorption at the vacancy site (Fig. 4d) is downhill by 0.70 eV. The adsorbed O_2 does not dissociate easily but reacts with CO to form a carbonate (Fig. 4e) and produce 3.24 eV of energy. This carbonate requires little energy to decompose into gaseous CO_2 and heal the oxygen vacancy. This sequence of reactions is also catalytic.

3.3. CO oxidation by the undoped CeO_2(111) surface

Infrared studies [94,95] of polycrystalline CeO_2 found that the surface exposed to CO contains weakly bound CO molecules and a variety of carbonates that decompose only at high temperature. XPS studies of CO adsorption on Ce(111) by Mullins and Overbury [96] identified carbonates and carboxylates on the surface.

Earlier calculations for CO adsorption provided conflicting results. The calculations of Yang et al. [69] concluded that carbonate forms on the (110) surface but not on (111). Later work [70] used periodic Hartree–Fock and DFT on small clusters and found no carbonate formation even on (110). Nolan et al. [67] calculated the binding energies pertinent to CO oxidation by the (111), (110), and (100) surfaces, by using LDA + U; however, that paper is a short communication that gives no information about the oxidation mechanism. Because we want to compare CO oxidation by the doped oxide with the oxidation by the pure oxide, we calculated the interaction of CO with CeO_2(111).

Previous computations by Yang et al. [69] did not find a stable carbonate when CO was adsorbed on CeO_2(111) surface. However, we find that CO reacts with a surface oxygen atom to form a CO_2 molecule which does not bind to the surface. The barrier for this reaction is at least 0.41 eV. (The barrier was obtained using the elastic band method implemented in VASP and is approximate because of the limited number of points on the elastic band.)

We also explored the formation of a carbonate on this surface (Fig. 5a), by the reaction of CO with an $O_{t,Ce}$ atom and an $O_{b,Ce}$ atom. We found that a carbonate forms (Fig. 5b), but this reaction is endothermic by 0.41 eV. This value is comparable to our estimates of the barrier for the formation of a CO_2 molecule by the reaction of CO to $O_{t,Ce}$. When the carbonate is formed, the oxygen atom from the top layer is pulled out of the surface to form a vacancy (the dotted line in Fig. 5b). This vacancy formation is the most costly aspect of carbonate formation. Any surface modification that facilitates vacancy formation is likely to facilitate formation of the carbonate.

The carbonate decomposes by releasing CO_2 in the gas phase and leaving behind an oxygen vacancy (Fig. 5c). An O_2 molecule binds strongly to the vacancy (Fig. 5d), with an exothermicity of 2.73 eV. The adsorbed oxygen molecule is

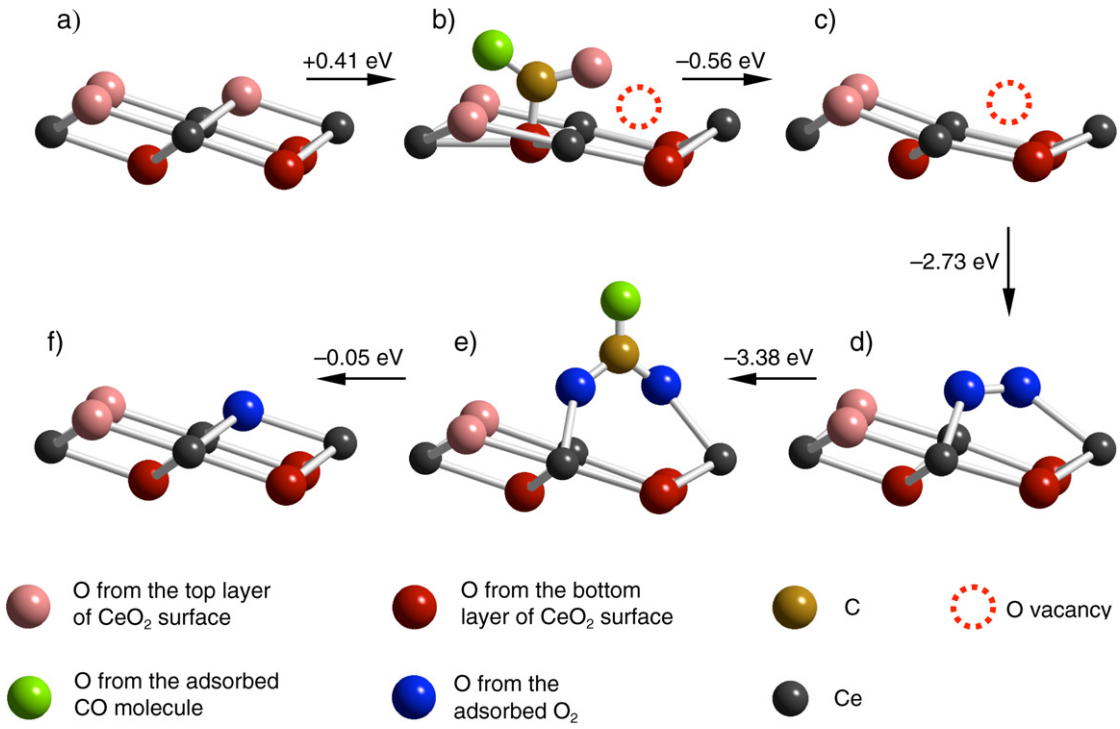

Fig. 5. Catalytic CO oxidation on pure CeO_2 surface: (a) clean surface; (b) formation of carbonate; (c) CO_2 desorbed leaving an O vacancy; (d) adsorption of O_2 at the vacancy; (e) formation of carbonate with adsorbed O_2; (f) CO_2 desorbed, clean surface restored.

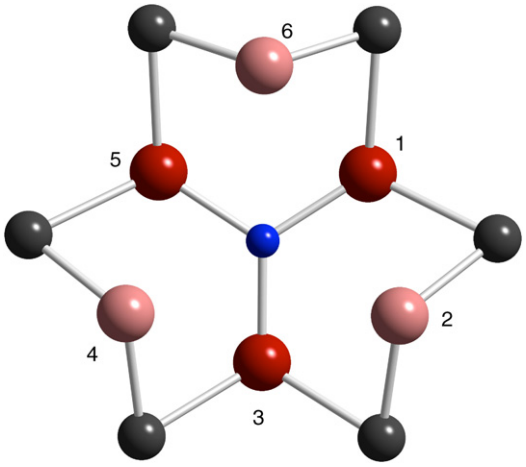

Fig. 6. The labels used in Table 1 to identify the oxygen atoms surrounding a given metal atom.

Table 1
Distances between the oxygen atoms O1 to O6 (see the labels in Fig. 6) and the dopant or the cerium atoms they bind to, in Å

	$Au_xCe_{1-x}O_2$		$Ag_xCe_{1-x}O_2$		$Cu_xCe_{1-x}O_2$		CeO_2
	O–Au	O–Ce	O–Ag	O–Ce	O–Cu	O–Ce	O–Ce
O1 (b)	2.372	2.379	2.409	2.397	2.090	2.517	2.386
O2 (t)	2.292	2.410	2.537	2.306	2.911	2.250	2.376
O3 (b)	2.372	2.379	2.410	2.397	2.039	2.464	2.386
O4 (t)	2.291	2.410	2.536	2.305	2.892	2.236	2.376
O5 (b)	2.372	2.379	2.409	2.397	2.092	2.514	2.386
O6 (t)	2.292	2.410	2.535	2.305	3.236	2.178	2.376

Note. Each oxygen atom binds to two cerium atoms and these two bonds are of equal length. The first two columns of numbers give distances for $Au_xCe_{1-x}O_2$, the next two for $Ag_xCe_{1-x}O_2$ and the last two for $Cu_xCe_{1-x}O_2$, and the last one gives the distances Ce–O distances in CeO_2. In Au_2O_3 the distances between the oxygen atoms and Au vary between 1.93 and 2.07 Å, the O–Ag distance in Ag_2O is 2.05 Å and the O–Cu in the Cu oxides (CuO and CuO_2) vary between 1.82 and 2.00 Å. The dopant–oxygen distance in doped ceria is much larger than the distance between the dopant and the oxygen in the dopant's own oxide.

weakened by the electron-rich environment at the vacancy site and reacts with CO to form a bridging carbonate (Fig. 5e) and release −3.38 eV of energy. The carbonate decomposes to produce CO_2 in the gas phase and heal the oxygen vacancy in the surface. This reaction is slightly exothermic (−0.05 eV). We conclude that the rate-limiting step in CO oxidation by $CeO_2(111)$ is the initial reaction of CO with the surface to form either a CO_2 molecule or a carbonate.

3.4. Doping with Ag and Cu

The disturbance caused by doping is reflected by the distance between the six oxygen atoms shown in Fig. 6 and the Ce and the dopant atoms in their neighborhood. Each of the oxygen atoms labeled in this figure is close to two cerium atoms, and the two cerium–oxygen distances are equal. Because of this, the table contains only one Ce–O distance. The table caption gives the oxygen–cerium distances in the undoped oxide and also the range of oxygen–metal distances in Au_2O_3, Ag_2O, and copper oxides (Cu_2O and CuO). In all cases, the dopant–oxygen distances in the doped oxide are substantially greater than those in the dopant's own oxide. In the Au and Ag compounds, the oxygen atoms surrounding the dopant maintain the three-fold symmetry. In the Cu compound, this symmetry is broken; the distance between Cu and O(6) is substantially larger that the

distances between Cu and O(4) and Cu and O(2). There is also a small symmetry breaking among the bottom oxygen atoms. The oxygen–cerium distances are disturbed substantially only in the $Cu_xCe_{1-x}O_2$ compound. The O_b atoms (1, 3, and 5 in Fig. 6) are further from Ce atoms in $Cu_xCe_{1-x}O_2$ than in CeO_2. The Ce distances to the O_t atoms are shorter in $Cu_xCe_{1-x}O_2$ than in CeO_2. We do not have any rationale for this behavior.

The EXAFS results of Bera et al. [40] indicate that Cu has three or four oxygen atoms in its first coordination shell, located at a distance of 1.96 Å. This is very different from the values that we obtained for the dopant in the outermost layer of the (111) face. This discrepancy may have a simple explanation. Wang et al. [97] found that the Cu atom in the bulk has four oxygen atoms next to it at a distance of 1.92–1.95 Å. Thus, it is possible that most of the EXAFS signal reported by Bera et al. [40] came from Cu atoms inside the material, not at the surface.

Previous work on doped titania [39], and recent unpublished work in our group, has shown that Zr, Hf, Ru, Sn, Mn, Ni, Pd, Pt, Cu, Ag, and Au dopants weaken the bond between the surface oxygen atoms and rutile TiO_2 (Chretien and Metiu, unpublished data) and that Na, K, Rb, Cs, Ni, Cu, Rh, Pd, Ag, Cd, Ir, Pr, and Au dopants have the same effect on ZnO (Pala and Metiu, unpublished data). However, Mg, Ca, Sr, Sc, Y, La, Ti, Zr, Hf, Ce, V, Nb, Ta, Cr, Mo, W, Mn, Re, Ru, Os, Co, Al, Ga, Sn, and Pb have the opposite effect (Pala and Metiu, unpublished data). An essential step in the Mars–van Krevelen oxidation mechanism is the reaction of a surface oxygen atom with a gas-phase reducing agent, to form an oxidation product and an oxygen vacancy on the surface. The high energy required for forming an oxygen vacancy is one reason why oxides perform oxidation reactions at high temperature. We expect that the dopant lowers the oxidation temperature by weakening the bond between the oxygen and the oxide. Thus, we can measure the oxidizing capacity of an oxide by calculating the energy needed to form a vacancy. However, it is important to keep in mind that this is not a measure of catalytic activity, because a second important step is the ability to heal the vacancy formed by the oxidation process by adsorbing and activating oxygen from the gas phase.

Table 2 gives the energy of oxygen-vacancy formation at the surface of ceria doped with Au, Ag, and Cu. The stability of the Cu oxide is greater than that of Ag, which in turn is greater than that of Au. Naively, one would expect that forming a vacancy in Au-doped ceria would require the least energy and that the oxygen atoms in the Cu-doped compound would be less willing to leave the oxide. But instead we find the opposite trend: Removing an oxygen atom from the Cu-doped ceria releases more energy than the same process on $Ag_xCe_{1-x}O_2$ or $Au_xCe_{1-x}O_2$.

By comparing the effects of various elements on the energy of vacancy formation in doped TiO_2 or CeO_2, we have found that two factors are the most important. A dopant with a lower valence than the cation that it replaces creates an electron deficit in its neighborhood. This weakens the bond between the oxide and the oxygen atoms in the neighborhood of the dopant. In addition, a dopant disrupts the oxygen–oxide bond if its own oxide has a different structure than that of the host. The dopant finds that the number of oxygen atoms in its neighborhood and

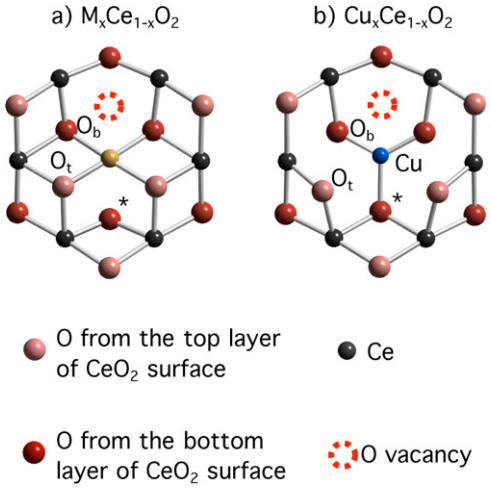

Fig. 7. The structure of the doped oxide after the removal of one O_t atom to form an oxygen vacancy at the surface (the dotted circle). (a) $M_xCe_{1-x}O_2$, M = Au, Ag; (b) $Cu_xCe_{1-x}O_2$. The creation of the vacancy breaks the symmetry and the oxygen atom marked by a star is different from the other O_b atoms.

Table 2
The distance between the dopant and various oxygen atoms after the oxygen vacancy shown in Fig. 7 has been made

	$Au_xCe_{1-x}O_2$	$Ag_xCe_{1-x}O_2$	$Cu_xCe_{1-x}O_2$
E_{vac}, eV	−0.36	−0.51	−0.83
Distance M–O_t, Å	2.35	2.47	3.17
Distance M–O_b, Å	2.33	2.40	2.07
Distance M–O*, Å	2.77	2.60	2.34

Note. The labels of the oxygen atoms were defined in Fig. 5 and in the text. E_{vac} is the energy needed to form one oxygen vacancy and half and oxygen molecule in the gas phase.

their positions are not "right" and has difficulties bonding to them. We propose that whenever one of these two factors is present, the dopant makes the surface oxygen more reactive and lowers the temperature at which the oxide is reduced.

Several observations by Bera et al. [40] are consistent with our results. They found that the concentration of the Cu atoms at the surface of $Cu_xCe_{1-x}O_2$ is four to six times higher that what would be derived by assuming that the Cu atoms initially introduced in the system take surface or bulk sites with equal probability. We find that the system has lower energy when the dopant is located in the surface layer. Bera et al. also found that the doped material has more vacancies than the undoped one, consistent with the substantial weakening of the oxygen–oxide bond found in our calculations. Finally, their temperature-programmed reduction (TPR) measurements indicated that Cu-doped ceria oxidizes hydrogen at lower temperature than CuO or ceria. Again, this agrees with our finding that removing oxygen atoms from the doped surface is easier than removing them from ceria.

4. Discussion

Because we have calculated only the total energy of the reactants, products, and intermediates involved in the catalytic oxidation of CO, we can discuss only the equilibrium behav-

ior of the system. We have found three important processes: (1) CO forms several carbonates by reacting with different pairs of oxygen atoms on the $Au_xCe_{1-x}O_2$ surface; some of these carbonates are fairly stable and will be present on the surface during the catalytic reaction; (2) other carbonates readily decompose to produce CO_2 and form an oxygen vacancy on the surface; and (3) the oxygen vacancies adsorb O_2, and this reacts with CO to form a carbonate that decomposes into CO_2 and leaves an oxygen atom behind to heal the vacancy.

We performed these calculations to explore whether doping an oxide improves its ability to perform oxidation reactions. We use the oxidation of CO by gold-doped ceria as an example. An important question is the extent to which the features discovered in our previous work [39] and in the present study can be extended to other systems. Although extrapolating chemical behavior is not a safe endeavor, we wish to emphasize several features that may be general. We find that doped oxides catalyze oxidation through a Mars–van Krevelen mechanism. The dopant weakens the bond between the oxide and the oxygen atoms at its surface, making them more reactive. In an oxidation reaction, the compound being oxidized takes an oxygen atom from the surface and creates an oxygen vacancy. Gas-phase O_2 adsorbs on the vacancy and is activated by the electron-rich environment that it finds there. One atom in this activated O_2 oxidizes a gas-phase molecule, and the other heals the oxygen vacancy in the surface. The oxygen atom activated by the presence of the dopant also might initiate a dehydrogenation reaction by taking a hydrogen atom from a gas-phase molecule to form a hydroxyl.

In this scenario, doping improves the catalytic properties of the surface if it satisfies two conflicting requirements. On the one hand, it must weaken the bond of the oxygen atoms to the oxide surface to allow the oxidation of the gas-phase reactant; on the other hand, this weakening must not be so pronounced that the vacancy can not be healed by reaction with gas-phase oxygen. TPR measurements of the threshold for CO or H_2 oxidation, in the absence of gas-phase oxygen, probe the ability of surface oxygen to react with the reducing molecules. Our calculations and several experimental studies have shown that doping lowers this threshold substantially. But TPR studies of reduction by hydrogen are not enough; obtaining complete information on the catalytic properties requires either studying a specific catalytic reaction or performing reoxidation experiments [98] along with TPR. Unless reoxidation is also effective, the doped oxide will not be a good oxidation catalyst. This may explain why some experiments [40–49] found that doping lowered the threshold temperature for oxide reduction, whereas others [54,55] found that doping lowered the catalytic activity in specific oxidation reactions. Note, however, that these "conflicting" experiments were performed on different doped oxides, which were obtained by different methods of preparation and likely had different morphologies.

In the case of ceria doped with Au, the energy to form a vacancy (half the energy of a gas-phase O_2 molecule, plus the energy of doped ceria with an oxygen vacancy, minus the energy of doped ceria) is -0.36 eV if the $O_{t,Au}$ is removed and $+0.56$ eV if $O_{t,Ce}$ is removed. The energy of forming an oxygen vacancy in undoped CeO_2 is $+3.01$ eV. It is clear that thermodynamics favors vacancy formation in doped ceria. However, the rate of vacancy formation in the absence of a reducing agent is likely to be very low because the distance between the oxygen atoms in ceria is larger than the O–O bond in O_2. This means that a concerted process by which two O atoms in the oxide will come together to form an O_2 molecule (which desorbs) and two vacancies will require a large activation energy. This is also true if an oxygen atom breaks its bonds with the oxide and moves on the surface to react with another surface-oxygen atom. Nevertheless, the fact that vacancy formation in the doped oxide is exothermic suggests that the oxygen atoms nearest and next-nearest the Au dopant are chemically active and that in the absence of an oxidizing atmosphere, the surface of a doped oxide has more oxygen vacancies than the pure host.

At this time, we are not sure which doped compounds can be synthesized and which are stable under reaction conditions. We speculate that in many cases $M_xN_{n-x}O_m$ is less stable than the two separated oxides. In the absence of oxygen in the gas phase, $M_xN_{n-x}O_m$ may be even less stable than a system consisting of metal clusters of M on N_nO_m. However, $M_xN_{n-x}O_m$ might be prepared if the synthesis is carried out so that the minority cation M gets trapped in the lattice of the host oxide N_nO_m as the latter is being formed and substitutes an N atom.

The fate of the dopant at the surface of the material under reaction conditions is not yet clear. In some experiments, it was observed that the ionic gold turns into Au^0 during CO oxidation or the water–gas shift reaction. We speculate that this occurs because the reducing agent removes oxygen atoms located near the dopant and this will make the dopant less positive. This may shift the XPS spectrum to make it look very similar to that of metallic M. If after the removal of oxygen atoms in its neighborhood the dopant is mobile, then it may migrate, meet other dopants, and form metallic clusters of M. If this happens it is likely that the process cannot be reversed by heating in oxygen, because this is likely to create an oxide cluster of M, with different chemical properties than those of the doped oxide. The process of reduction can be prevented if oxygen is present in the gas phase in sufficient quantity to replace the oxygen lost through the reduction process at a sufficiently fast rate. Flytzani-Stephanopoulos et al. [14,15] have shown that reduction of the Au dopant during the water–gas shift reaction can be stopped by adding oxygen into the feed stream. Hegde's [40] and Rodriguez's [97] groups have shown that temperature programmed hydrogen reduction turns Cu, in $Cu_xCe_{1-x}O_2$, into Cu^0 and that subsequent exposure to oxygen at high temperature recovers $Cu_xCe_{1-x}O_2$. Both experiments revealed that this reoxidation of Cu^0 did not lead to a copper oxide and that $Cu_xCe_{1-x}O_2$ was recovered. We speculate that this would not happen if Cu^0 formed metal clusters, because these would be oxidized to form a copper oxide. One possibility is that the reduced Cu atoms do not leave the site where they were located in $Cu_xCe_{1-x}O_2$ and that removing some of the adjacent oxygen atoms makes them appear to be Cu^0 in the XPS signal. When the reduced surface is exposed to gas-phase oxygen, the lost oxygen atoms are recovered, and the XPS spectrum is now that of $Cu_xCe_{1-x}O_2$. Unfortunately, the XPS experiments

probe some of the Cu atoms in the bulk. These may lose oxygen on reduction with hydrogen and not have sufficient mobility to lose the site in which they are located. On heating under oxygen pressure, they recover the lost oxygen, and their XPS spectrum returns to that before reduction.

Doped oxides are of interest for low-temperature oxidation reactions, and thus their stability may not be a critical issue. In favorable cases, doping improves the thermal stability of the catalyst; Pd-doped perovskite is more stable than Pd supported on an oxide [50–53].

It is often suggested that oxygen vacancies are chemically active and play an important role in catalysis. We find that the oxygen vacancies on the surface of doped ceria are chemically active, adsorb O_2, and use it to form a carbonate, which decomposes to form CO_2 and annihilate the vacancy. But this chain of reactions is not catalytic; it starts at a vacancy site and causes the vacancy to disappear. The reduced oxide is not an oxidation catalyst unless a vacancy-making reaction is also present.

Our model contains a number of simplifications and uncertainties. DFT may have difficulty providing accurate results for an oxide with narrow f-bands. However, to invalidate the trends predicted here, these errors would have to be very large so that they would not cancel when we calculated the energy differences of interest to chemistry. Because of this, we believe that our qualitative conclusions are correct and that most dopants will increase the oxidative power of the host oxide.

Many experimental papers have emphasized that the activity of the doped oxides seems to be enhanced when the oxide has a higher surface area. The (111) face of ceria has the lowest surface energy, and one could argue that it will be most common facet in the dispersed oxide. This assumption is supported by TEM and SEM images of the CeO_2 powders of various sizes [99,100]. However, a dispersed oxide has a large number of kinks and steps and other low-coordination sites. We have not explored how such sites affect catalytic activity.

Acknowledgments

Calculations were performed at the California NanoSystems Institute (CNSI) computer facilities funded by the National Science Foundation under grant CHE-0321368. This work was supported by the Air Force Office of Scientific Research under contracts F49620-01-1-0459 and FAA9550-06-1-0167.

References

[1] D. Andreeva, Gold Bull. 35 (2002) 82.
[2] D. Andreeva, V. Idakiev, T. Tabakova, L. Ilieva, P. Falaras, A. Bourlinos, A. Travlos, Catal. Today 72 (2002) 51.
[3] D. Andreeva, I. Ivanov, L. Ilieva, M.V. Abrashev, Appl. Catal. A 302 (2006) 127.
[4] T. Tabakova, F. Boccuzzi, M. Manzoli, J.W. Sobczak, V. Idakiev, D. Andreeva, Appl. Catal. B 49 (2004) 73.
[5] T. Tabakova, F.B. Boccuzzi, M. Manzoli, D. Andreeva, Appl. Catal. A 252 (2003) 385.
[6] T. Tabakova, F. Boccuzzi, M. Manzoli, J.W. Sobczak, V. Idakiev, D. Andreeva, Appl. Catal. A 298 (2006) 127.
[7] F. Boccuzzi, A. Chiorino, M. Manzoli, D. Andreeva, T. Tabakova, J. Catal. 188 (1999) 176.
[8] F. Boccuzzi, A. Chiorino, M. Manzoli, D. Andreeva, T. Tabakova, L. Ilieva, V. Iadakiev, Catal. Today 73 (2002) 169.
[9] Q. Fu, A. Weber, M. Flytzani-Stephanopoulos, Catal. Lett. 77 (2001) 87.
[10] Q. Fu, H. Saltsburg, M. Flytzani-Stephanopoulos, Science 301 (2003) 935.
[11] Q. Fu, S. Kudriavtseva, H. Saltsburg, M. Flytzani-Stephanopoulos, Chem. Eng. J. (Amsterdam) 93 (2003) 41.
[12] X. Qi, M. Flytzani-Stephanopoulos, Ind. Eng. Chem. Res. 43 (2004) 3055.
[13] W. Deng, J.D. Jesus, H. Saltsburg, M. Flytzani-Stephanopoulos, Appl. Catal. A 291 (2005) 126.
[14] W.L. Deng, M. Flytzani-Stephanopoulos, Angew. Chem. Int. Ed. 45 (2006) 2285.
[15] Q. Fu, W. Deng, H. Saltsburg, M. Flytzani-Stephanopoulos, Appl. Catal. B 56 (2005) 57–68.
[16] X. Wang, J.A. Rodriguez, J.C. Hanson, M. Perez, J. Evans, J. Chem. Phys. 123 (2005) 221101.
[17] G. Avgouropoulos, T. Ioannides, C. Papadopoulou, J. Batista, S. Hocevar, H.K. Matralis, Catal. Today 75 (2002) 157.
[18] G.K. Bethke, H.H. Kung, Appl. Catal. A 194 (2000) 43.
[19] C.K. Costello, J.H. Yang, H.Y. Law, Y. Wang, J.N. Lin, L.D. Marks, M.C. Kung, H.H. Kung, Appl. Catal. A 243 (2003) 15.
[20] S.D. Gardner, G.B. Hoflund, D.R. Schryer, J. Schryer, B.T. Upchurch, E.J. Kielin, Langmuir 7 (1991) 2135.
[21] O. Goerke, P. Pfeifer, K. Schubert, Appl. Catal. A 263 (2004) 11.
[22] M. Haruta, S. Tsubota, T. Kobayashi, H. Kageyama, M.J. Genet, B. Delmon, J. Catal. 144 (1993) 175.
[23] M. Haruta, N. Yamada, T. Kobayashi, S. Iijima, J. Catal. 115 (1989) 301.
[24] L. Kundakovic, M. Flytzani-Stephanopoulos, J. Catal. 179 (1998) 203.
[25] W. Liu, M. Flytzanis-tephanopoulos, J. Catal. 153 (1995) 317.
[26] A. Luengnaruemitchai, S. Osuwan, E. Gulari, Catal. Commun. 4 (2003) 215.
[27] A. Luengnaruemitchai, S. Osuwan, E. Gulari, Int. J. Hydrogen Energy 29 (2004) 429.
[28] M. Manzoli, A. Chiorino, F. Boccuzzi, Appl. Catal. B 52 (2004) 259.
[29] G. Panzera, V. Modafferi, S. Candamano, A. Donato, F. Frusteri, P.L. Antonucci, J. Power Sources 135 (2004) 177.
[30] M.M. Schubert, V. Plzak, J. Garche, R.J. Behm, Catal. Lett. 76 (2001) 143.
[31] M.M. Schubert, A. Venugopal, M.J. Kahlich, V. Plzak, R.J. Behm, J. Catal. 222 (2004) 32.
[32] B. Schumacher, Y. Denkwitz, V. Plzak, M. Kinne, R.J. Behm, J. Catal. 224 (2004) 449.
[33] T. Tabakova, V. Idakiev, K. Tenchev, F. Boccuzzi, M. Manzoli, A. Chiorino, Appl. Catal. B 63 (2006) 94.
[34] S. Carrettin, P. Concepcion, A. Corma, J.M. Lopez Nieto, V.F. Puntes, Angew. Chem. Int. Ed. 43 (2004) 2538.
[35] S. Carrettin, A. Corma, M. Iglesias, F. Sanchez, Appl. Catal. A Gen. 291 (2005) 247.
[36] J. Guzman, S. Carrettin, A. Corma, J. Am. Chem. Soc. 127 (2005) 3286.
[37] A.M. Venezia, G. Pantaleo, A. Longo, G. Di Carlo, M.P. Casaletto, F.L. Liotta, G. Deganello, J. Phys. Chem. B 109 (2005) 2821.
[38] X. Zhang, H. Shi, B.Q. Xu, Angew. Chem. Int. Ed. 44 (2005) 7132.
[39] S. Chretien, H. Metiu, Catal. Lett. 107 (2006) 143.
[40] P. Bera, K.R. Priolkar, P.R. Sarode, M.S. Hegde, S. Emura, R. Kumashiro, N.P. Lalla, Chem. Mater. 14 (2002) 3591.
[41] P. Bera, S. Malwadkarb, A. Gayena, C.V.V. Satyanarayanab, B.S. Raob, M.S. Hegde, Catal. Lett. 96 (2004) 213.
[42] P. Bera, K.R. Priolkar, A. Gayen, P.R. Sarode, M.S. Hegde, S. Emura, R. Kumashiro, V. Jayaram, G.N. Subbanna, Chem. Mater. 15 (2003) 2049.
[43] T. Baidya, A. Gayen, M.S. Hedge, N. Ravishankar, L. Dupont, J. Phys. Chem. B 110 (2006) 5262.
[44] A. Gayen, K.R. Priolkar, R. Sarode, V. Jayaram, M.S. Hegde, G.N. Subbanna, S. Emura, Chem. Mater. 16 (2004) 2317.
[45] F.J. Perez-Alonso, I. Melian-Cabrera, M. Loper Granados, F. Kapteijs, J.L.G. Fierro, J. Catal. 239 (2006) 340.
[46] T.B. Nguyen, J.P. Deloume, V. Perrichon, Appl. Catal. A Gen. 249 (2003) 273–284.

[47] K. Nagaveni, M.S. Hegde, G. Madras, J. Phys. Chem. B 108 (2004) 20204.
[48] W. Shan, Z. Feng, Z. Li, J. Zhang, W. Shen, C. Li, J. Catal. 228 (2004) 206.
[49] W.J. Shan, W.J. Shen, C. Li, Chem. Mater. 15 (2003) 4761.
[50] M. Misono, Catal. Today 100 (2005) 95.
[51] Y. Nishihata, J. Mizuki, T. Akao, H. Tanaka, M. Uenishi, M. Kimura, T. Okamoto, N. Hamada, Nature 418 (2002) 164.
[52] H. Tanaka, N. Mizuno, M. Misono, Appl. Catal. A 244 (2003) 371.
[53] H. Tanaka, I. Tan, M. Uenishi, M. Kimura, K. Dohmae, Top. Catal. 16/17 (2001) 63.
[54] S. Zhao, R.J. Gorte, Appl. Catal. A 248 (2003) 9.
[55] M.F. Wilkes, P. Hayden, A.K. Bhattacharya, J. Catal. 219 (2003) 295.
[56] S. Fabris, S. De Gironcoli, S. Baroni, G. Vicario, G. Balducci, Phys. Rev. B Condens. Matter Mater. Phys. 71 (2005) 041102.
[57] S. Fabris, S. De Gironcoli, S. Baroni, G. Vicario, G. Balducci, Phys. Rev. B 72 (2005) 237102.
[58] S. Fabris, G. Vicario, G. Balducci, S. De Gironcoli, S. Baroni, J. Phys. Chem. B 109 (2005) 22860.
[59] N.V. Skorodumova, R. Ahuja, S.I. Simak, I.A. Abrikosov, B. Johansson, B.I. Lundqvist, Phys. Rev. B Condens. Matter Mater. Phys. 64 (2001) 115108.
[60] B. Herschend, M. Baudin, K. Hermansson, Surf. Sci. 599 (2005) 173.
[61] N.V. Skorodumova, M. Baudin, K. Hermansson, Phys. Rev. B Condens. Matter Mater. Phys. 69 (2004) 075401.
[62] N.V. Skorodumova, S.I. Simak, B.I. Lundqvist, I.A. Abrikosov, B. Johansson, Phys. Rev. Lett. 89 (2002) 166601.
[63] Y. Jiang, J.B. Adams, M. Van Schilfgaarde, J. Chem. Phys. 123 (2005) 064701.
[64] G. Kresse, P. Blaha, J.L.F. Da Silva, M.V. Ganduglia-Pirovano, Phys. Rev. B 72 (2005) 237101.
[65] F. Esch, S. Fabris, L. Zhou, T. Montini, C. Africh, P. Fornasiero, G. Comelli, R. Rosei, Science 309 (2005) 752.
[66] M. Nolan, S. Grigoleit, D.C. Sayle, S.C. Parker, G.W. Watson, Surf. Sci. 576 (2005) 217.
[67] M. Nolan, S.C. Parker, G.W. Watson, Phys. Chem. Chem. Phys. 8 (2006) 216.
[68] A. Gotte, K. Hermansson, M. Baudin, Surf. Sci. 552 (2004) 273.
[69] Z. Yang, T.K. Woo, K. Hermansson, Chem. Phys. Lett. 396 (2004) 384.
[70] C. Mueller, C. Freysoldt, M. Baudin, K. Hermansson, Chem. Phys. 318 (2005) 180.
[71] V.I. Anisimov, F. Aryasetiawan, A.I. Lichtenstein, J. Phys. Condens. Matter 9 (1997) 767.
[72] V.I. Anisimov, O. Gunnarsson, Phys. Rev. B 43 (1991) 7570.
[73] V.I. Anisimov, I.V. Solovyev, M.A. Korotin, M.T. Czyzyk, G.A. Sawatzky, Phys. Rev. B 48 (1993) 16929.
[74] V.I. Anisimov, J. Zaanen, O.K. Andersen, Phys. Rev. B 44 (1991) 943.
[75] I.V. Solovyev, P.H. Dederichs, V.I. Anisimov, Phys. Rev. B 50 (1994) 16861.
[76] A.I. Liechtenstein, V.I. Anisimov, J. Zaanen, Phys. Rev. B 52 (1995) R5467.
[77] W.E. Pickett, S.C. Erwin, E.C. Ethridge, Phys. Rev. B 58 (1998) 1201.
[78] E. Antonides, E.C. Janse, G.A. Sawatzky, Phys. Rev. B 15 (1977) 1669.
[79] O. Bengone, M. Alouani, P. Blochl, J. Hugel, Phys. Rev. B 62 (2000) 16392.
[80] M. Cococcioni, S. De Gironcoli, Phys. Rev. B 71 (2005).
[81] D. Van Der Marel, G.A. Sawatzky, F.U. Hillebrecht, Phys. Rev. Lett. 53 (1984) 206.
[82] G. Pacchioni, F. Frigoli, D. Ricci, J.A. Weil, Phys. Rev. B 63 (2001) 54102.
[83] A. Rohrbach, J. Hafner, Phys. Rev. B 71 (2005) 45405.
[84] A. Rohrbach, J. Hafner, G. Kresse, Phys. Rev. B 69 (2004) 75413.
[85] M. Lintuluoto, Y. Nakamura, J. Mol. Struct. Theochem 674 (2004) 207.
[86] J. Zuo, R. Pandey, A.B. Kunz, Phys. Rev. B 44 (1991) 7187.
[87] R.L. Putnam, A. Navrotsky, E.H.P. Cordfunke, M.E. Huntelaar, J. Chem. Thermodyn. 32 (2000) 911.
[88] H.L. Johnston, M.K. Walker, J. Am. Chem. Soc. 55 (1933) 172.
[89] P. Bera, M.S. Hegde, Catal. Lett. 79 (2002) 75.
[90] G. Kresse, J. Furthmller, Comput. Mater. Sci. 6 (1996) 15.
[91] G. Kresse, J. Furthmuller, Phys. Rev. B 54 (1996) 11169.
[92] G. Kresse, J. Hafner, Phys. Rev. B 47 (1993) 558.
[93] G. Kresse, J. Hafner, Phys. Rev. B 49 (1994) 14251.
[94] F. Bozon-Verduraz, A. Bensalem, J. Chem. Soc. Faraday Trans. 90 (1994) 653.
[95] C. Li, Y. Sakata, T. Arai, K. Domen, K. Maruya, T. Onishi, J. Chem. Soc. Faraday Trans. I 85 (1989) 924.
[96] D.R. Mullins, S.H. Overbury, J. Catal. 188 (1999) 340.
[97] X. Wang, J.A. Rodriguez, J.C. Hanson, D. Gamarra, A. Martinez-Arias, M. Fernandez-Garcia, J. Phys. Chem. B 109 (2005) 19595.
[98] M. Boaro, F. Giordano, S. Recchia, V.D. Santo, M. Giona, A. Trovarelli, Appl. Catal. B 52 (2004) 225.
[99] Z.L. Wang, X. Feng, J. Phys. Chem. B 107 (2003) 13563.
[100] E. Aneggi, J. Llorca, M. Boaro, A. Trovarelli, J. Catal. 234 (2005) 88.